

Description of catchment hydrological response using the catchment area function

SRIKANTHA HERATH, DAWEN YANG & KATUMI MUSIAKE

Institute of Industrial Science, University of Tokyo, 7-22-1 Roppongi, Minato-ku, Tokyo 106, Japan

e-mail: herath@inccede.iis.u-tokyo.ac.jp

Abstract The catchment area function concept is utilized to transform two-dimensional spatial distributions of catchment characteristics to one-dimensional form. A physically based hillslope model utilizing this representation is coupled with a kinematic wave river flow model to describe the catchment hydrological response. The model is applied to two Japanese catchments, located in the north and south respectively, and simulates both long and short term catchment responses well. Normalized seasonal hillslope responses are found to be good indicators for describing catchment hydrological response characteristics. Similar analysis of two recent flood events in the catchments gives useful information on runoff generation area distribution.

INTRODUCTION

Topography, geology and climate are the three main factors determining the hydrological response of a catchment. Catchment geomorphology is also a function of these three parameters, and can be an indicator of the catchment hydrological response. In the past several investigators have studied catchment area function as a representation of the geomorphologic characteristics of a catchment (Rinaldo *et al.*, 1993; Yang *et al.*, 1997a). Robinson *et al.* (1995) used the area function to represent the hillslope response, and to integrate the river response to determine the catchment hydrological response. Mesa & Mifflin (1986) used the catchment width function as an approximation to the catchment area function. Naden (1992) used the width function to describe spatial variability of rainfall and soil properties and to derive a catchment hydrological model. Yang *et al.* (1997b) used the area function to describe the rainfall distribution for modelling floods by coupling it with the tank model. In this paper, we present a distributed numerical simulation system consisting of a physically based hillslope response model coupled with a river routing model to simulate catchment hydrological response. The model is used to simulate the hydrological response in two catchments in Japan, for a four-year period at hourly time steps, and the hydrological response characteristics are discussed.

METHODOLOGY

The hydrological model consists of a hillslope response component and a river flow routing component. The area function and the width function are used to separate the catchment into a number of hillslopes and the discharge from the hillslopes is routed

by the river flow model. The area function $A(x)$, is defined as the frequency distribution of the accumulative catchment area with respect to flow distance from the outlet and is given by $A(x) = dA_c(x)/dx$, where $A_c(x)$ is the total accumulative area which drains into a point at distance x from the catchment outlet. The width function, $W(x)$, is defined as the frequency distribution of streams with respect to flow distance from the outlet.

For hydrological modelling, the catchment is divided into a number of flow intervals. Considering any flow interval Δx at distance x , the catchment area accumulated in this interval is given by the area function. Catchment area within each flow interval is represented as a series of hillslopes where the number of hillslopes within a flow interval is given by the width function. Hillslope response computed at each hillslope element provides the lateral inflow to the river, which is a lumped representation of the river network. Total catchment response is derived by solving the river routing model.

Hillslope model

A hillslope element is assumed to be a rectangular inclined plane of width equivalent to the flow interval length Δx , length L and uniform surface slope α . The bed rock slope is assumed to be parallel to the surface (Fig. 1). The hillslopes are located symmetrically on both sides of the river. The hydrological processes on hillslope include interception, evapotranspiration, snow melt, infiltration, overland flow, unsaturated soil water flow and groundwater flow. Layers for canopy, soil surface and a number of soil zones parallel to the surface represent vertical plane from canopy to groundwater table.

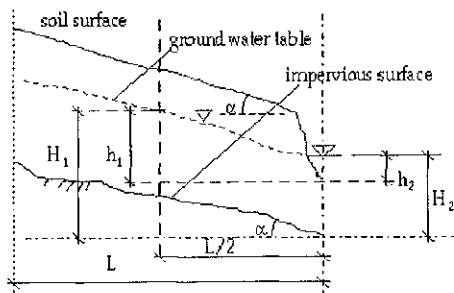


Fig. 1 Hillslope element.

Interception and evapotranspiration The interception capacity of the canopy depends on the vegetation coverage and the leaf-area-index. Actual interception is determined by the precipitation amount and the deficit of the canopy water storage. Interception capacity and the deficit of canopy water storage are given by:

$$S_{c_d}(t) = I_0 K_v LAI(t) - S_c(t) \quad (1)$$

where, I_0 is the maximum interception ability of the vegetation in a year (mm); K_v is the fraction of vegetation coverage; LAI is the leaf-area-index, with the maximum as 1;

$S_{c_v}(t)$ is the deficit of canopy water storage (mm) and $S_c(t)$ is the canopy water storage (mm) at time t .

The potential evaporation is estimated using the radiation-based method due to availability of data. Actual evapotranspiration is calculated as the summation of evaporation from canopy water storage (E_{canopy}), transpiration from the root zone (E_{tr}), evaporation from surface storage ($E_{surface}$) and evaporation from the soil surface (E_s), given by the following equations:

$$\begin{aligned}
 E_{canopy}(t)\Delta t &= \begin{cases} E_p \Delta t, & S_c(t) \geq E_p \Delta t \\ S_c(t), & S_c(t) < E_p \Delta t \end{cases} \\
 E_{in}(t, i) &= (K_c E_p - E_{canopy}(t)) K_v f_1(z_i) f_2(\theta) LAI(t) \\
 E_{surface}(t)\Delta t &= \begin{cases} E_p(1 - K_v)\Delta t, & S_s(t) \geq E_p(1 - K_v)\Delta t \\ S_s(t), & S_s(t) < E_p(1 - K_v)\Delta t \end{cases} \\
 E_s(t)\Delta t &= (E_p(1 - K_v) - E_{surface}) f_2(0)
 \end{aligned} \tag{2}$$

where, E_p is the potential evaporation rate (mm h^{-1}); Δt is the time interval (h); K_c is the crop coefficient; f_1 is the root distribution function; $S_s(t)$ is the surface water storage (mm) at time t ; and $f_2(\theta)$ is taken to vary linearly from 0 to 1 for θ from θ_r to θ_f (moisture content at field capacity) and to be 1 for $\theta > \theta_f$.

Snow melt Snow melting is simulated using a modified degree-day model. The degree-day snow melting factor is calibrated from recorded data. Considering the effective day time as 12 h, the degree-day factor is divided by 12 h to convert to degree-hour factor. The snow melting rate is given as:

$$M_s(t) = D_f(T(t) - T_b) \tag{3}$$

where, $M_s(t)$ is the snow melting rate (mm h^{-1}) at time t ; D_f is the degree-hour factor ($\text{mm degree}^{-1} \text{h}^{-1}$); $T(t)$ is the air temperature (degree) at time t and T_b is the base temperature when snow starts to melt (degree).

Surface runoff and infiltration The runoff is computed considering the mass balance for the surface storage given by:

$$\Delta S_s(t + \Delta t) / \Delta t = P_n(t) + M_s(t) - q_s(t) - f_{in}(t) - E_{surface}(t) \tag{4}$$

where $\Delta S_s(t + \Delta t)$ is the change of surface water storage (mm) at time t during time duration Δt ; $P_n(t)$ is net rainfall intensity (mm h^{-1}) at time t ; $f_{in}(t)$ is the infiltration rate (mm h^{-1}) at time t , which is calculated as:

$$f_{in}(t) = K_0 \text{ for } P_n(t) \geq K_0 \text{ and } f_{in}(t) = P_n(t) \text{ for } P_n(t) < K_0 \tag{5}$$

where, K_0 is the saturated hydraulic conductivity (mm h^{-1}). $q_s(t)$ is the surface runoff (mm h^{-1}), calculated by:

$$q_s(t)\Delta t = \begin{cases} S(t) - S_{\max}, & S(t) > S_{\max} \\ 0, & S(t) \leq S_{\max} \end{cases} \tag{6}$$

in which, $S(t)$ is the surface water storage (mm) at time t and S_{max} is the maximum surface storage (mm).

Unsaturated zone (multi-layer model) The top unsaturated soil is divided into a number of layers and the mass balance equation for layer i is given by:

$$\Delta S_{sub_i}(t + \Delta t) / \Delta t = f_{i-1}(t) - f_i(t) - E_{tr,i}(t) - E_{s_i}(t) \quad (7)$$

where, ΔS_{sub_i} is the change of water storage (mm) in layer i at time t during time interval Δt ; $f_i(t)$ is the recharge rate from layer i to layer $i + 1$, (mm h^{-1}). $f_i(t)$ ($i > 0$) is given by:

$$f_i(t) = \begin{cases} K(\theta_i), & \theta_i > \theta_f \text{ or } \theta_{i+1} \leq \theta_i \\ 0, & \theta_i \leq \theta_f \text{ and } \theta_{i+1} > \theta_i, z_{i+1} > z_i \end{cases} \quad (8)$$

in which, θ_i is the soil moisture content in layer i ; θ_f is the field moisture capacity and $K(\theta_i)$ is the hydraulic conductivity (mm h^{-1}). In equation (8) the matrix potential is neglected and the infiltration process is estimated as gravity flow which is reasonable for humid regions (Ni et al., 1994).

Saturated zone and exchange with the river The basic equations used for the saturated zone are mass balance and Darcy's law. The mass balance for hillslope aquifer segment is given by:

$$\Delta S_G(t + \Delta t) / \Delta t = rech(t) - L(t) - q_G(t) \frac{1000}{A} \quad (9)$$

where, $\Delta S_G(t + \Delta t)$ is the change of groundwater storage (unconfined aquifer) (mm); $rech(t)$ is the recharge rate from upper unsaturated zone (mm h^{-1}); $L(t)$ is the leakage to deep aquifer, (mm h^{-1}); A is the plane area of hillslope element, ($\text{m}^2 \text{m}^{-1}$) and $q_G(t)$ is the discharge to the river per unit width ($\text{m}^3 \text{h}^{-1} \text{m}^{-1}$), calculated using Darcy's law.

River routing

The kinematic wave model given by the continuity and momentum equations is used for river routing and solved using an explicit finite difference method.

$$\frac{\partial Q}{\partial x} + \frac{\partial A}{\partial t} = q_L, \quad q_L = q_S + q_G \quad (10)$$

where, x is the distance along the longitudinal axis of the river (m); t is time (s); A is the cross-sectional area (m^2); Q is the discharge at x ($\text{m}^3 \text{s}^{-1}$), given by Manning's equation.

STUDY AREA

Two catchments, the Naka River and the Seki River (Fig. 2) located in Shikoku and Hokuriku regions respectively were selected as the study area. The Naka River catchment

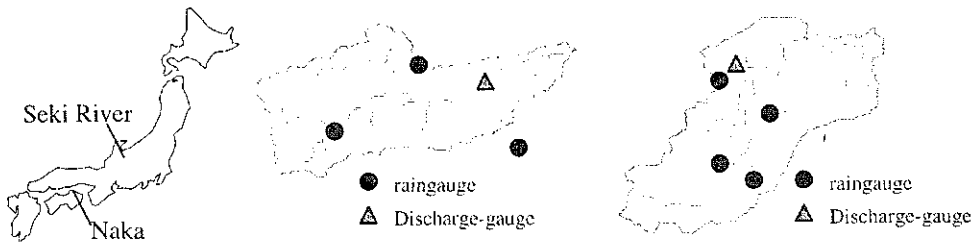


Fig. 2 Study area (left: the Naka River, right: the Seki River).

covers an area of 690 km^2 (above the discharge-measuring gauge) of which 90% is mountainous and has a main river length about 95 km. Three raingauges are available in (or near) this catchment. For the Seki River, the catchment area above the gauging point is 703 km^2 , the main river length is about 61 km and mountainous areas cover 80% of the total area. Four raingauges are available in the Seki River. Figure 3 shows the area functions of the two catchments. A digital elevation model (DEM) of 250 m mesh size was used to delineate the catchments, derive river network, the area function and to compute slope and elevation distributions. Elevation and slope distribution variation with flow distance, averaged at each flow interval, for the two catchments are shown in Fig. 4(a, b).

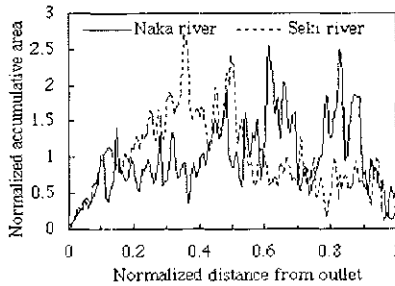


Fig. 3 Area function of the Naka River and the Seki River.

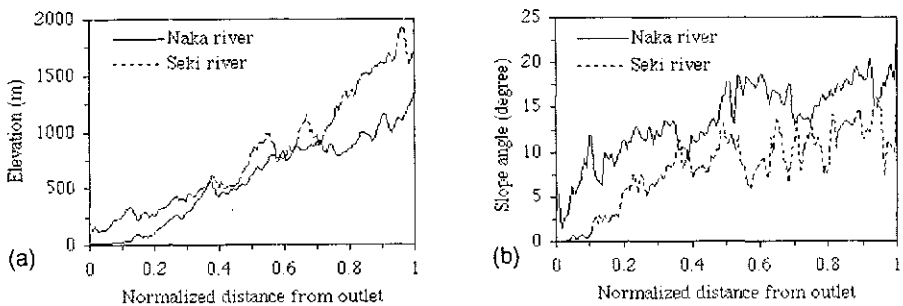


Fig. 4 Distributions of spatial variations: (a) elevation, (b) slope.

MODEL APPLICATION

Long-term continuous simulations were carried out for both catchments from 1992 to 1995. Considering the singularity spectrum of width function and area function for a

number of threshold areas (Yang *et al.*, 1997a), the critical values of the threshold areas were determined as 1.25 km² for the Naka River and 2.5 km² for the Seki River, and were used in deriving the area function and the width function from DEM. For the simulation, flow intervals were determined automatically such that the maximum interval is 800 m, and the interval is always less than the stream link length along the main river channel. This resulted in flow intervals ranging from 200–800 m. 119 flow intervals were used in the computations for the Naka River and 138 for the Seki River. The number of hillslope elements ranged from 1 to 10 per flow interval depending on the stream link density defined by the width function. Rainfall, temperature, slope and other physical parameters were also prepared as distributions with respect to flow distance, similar to the area function.

The catchments were treated as homogeneous with respect to land cover and soil distribution and the dominant category in each was used. Almost all the other parameters were estimated from catchment characteristics. For equivalent river in the model, Manning's roughness coefficient was assigned to be varying from 0.08 to 0.035 from the source to the outlet. The most important parameter to be calibrated was the saturated hydraulic conductivity K_0 , which was found to be 12 cm h⁻¹ for the Naka River basin and 10 cm h⁻¹ for the Seki River basin. The soil hydraulic properties were taken from measured data for the dominant soil group for each catchment. The hydrological data of year 1992 were used for model calibration and the rest of the period was used for validation.

The daily hydrographs of 1993 for both catchments are shown in Fig. 5(a,b). Enlarged view of the hydrographs describing two major flood events in the catchments, August 1993 in the Naka River and July 1995 in the Seki River, are given in Fig. 6(a,b). The simulation shows that the model is capable of simulating both short term and long term hydrological responses very well.

HYDROLOGICAL CHARACTERISTICS

In order to understand the catchment response, the hillslope response was accumulated with respect to the flow distance from catchment outlet, which facilitates comparison of the distribution with respect to the area function. The normalized yearly hillslope runoff (normalized by total runoff) and normalized area function (normalized by total area) are compared in Fig. 7(a,b).

The Naka River located in southern Japan is characterized by old rocks dating back from the Palaeozoic to Mesozoic era. As the catchment lies in a fault zone, the underlying rock formation is fractured and the groundwater yield is higher than that of similar geological origins. However, as characterized by the geological origins, its groundwater yield is still very small in comparison to the total hydrological response. Also the slope distribution does not vary much for about 90% of the catchment lying in the range of 10–20 degrees. The vegetation, land use and soil distributions are nearly uniform for the catchment. These conditions are reflected by the annual distribution of the hillslope response shown in Fig. 7(a) where the slope discharge is seen to be proportional to the area distribution. The seasonal variation of the hillslope response showed a distribution almost identical to the area function, as can be expected from uniform catchment characteristics and small groundwater contribution.

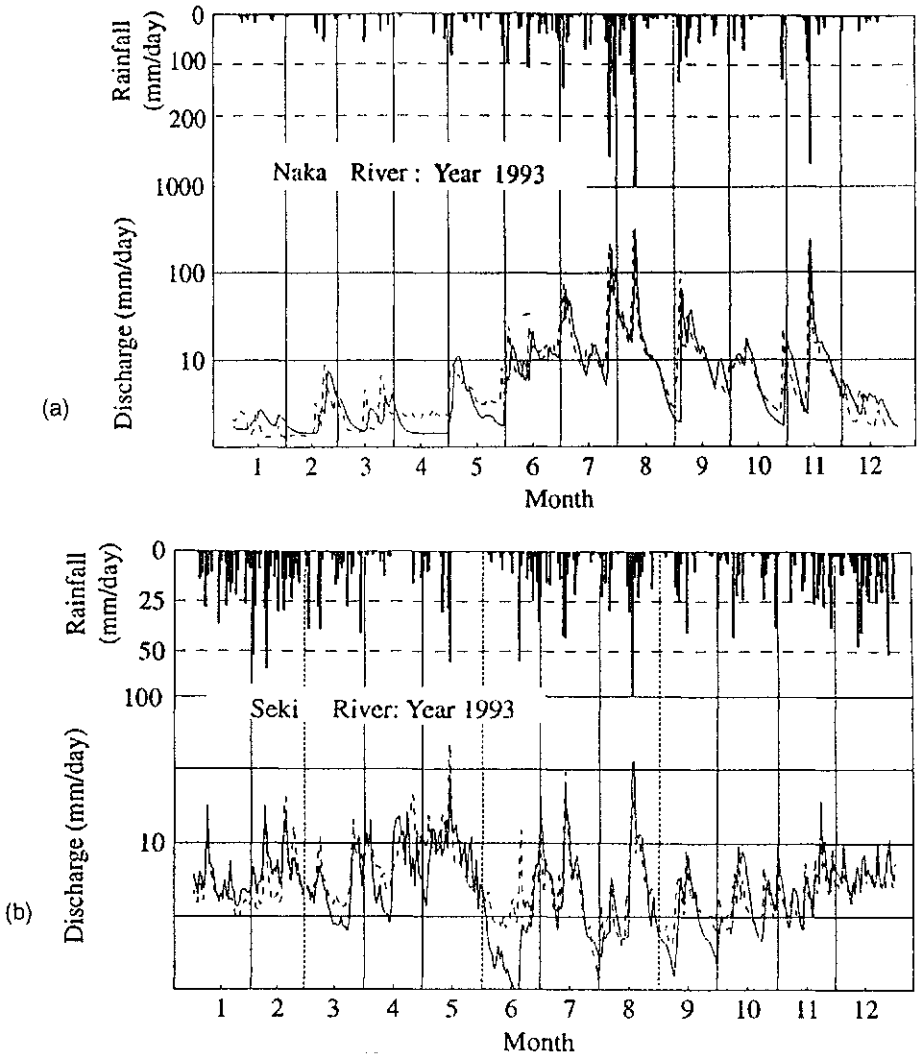


Fig. 5 Daily hydrographs (solid line: simulated; dashed line: observed) (a) Naka River (b) Seki River.

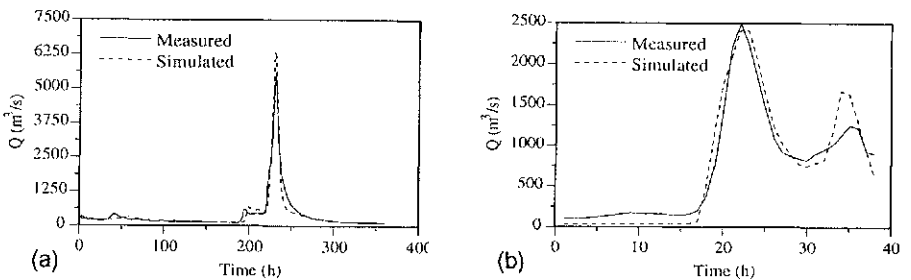


Fig. 6 Flood simulation: (a) Naka River (August 1-15, 1993), (b) Seki River (July 11-12, 1995).

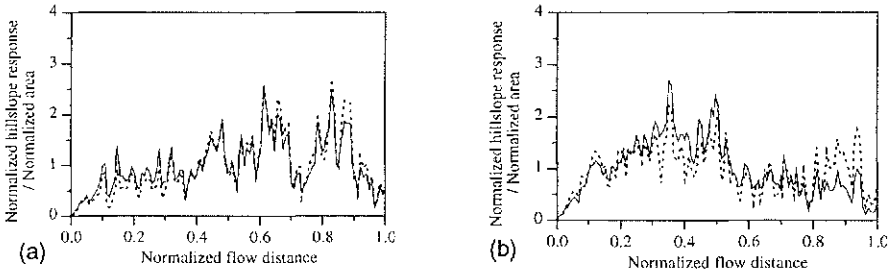


Fig. 7 Yearly hillslope response distribution comparison with area function: (a) Naka River (b) Seki River (solid line: normalized accumulative area; dashed line: normalized yearly hillslope response).

The Seki River catchment, located in northern Japan, which has porous soils of volcanic ash origin, is subjected to considerable snowfall. The annual hillslope response distribution in Fig. 7(b) shows that hillslope response contribution from the furthest locations of the catchment, in the range of 0.8–1.0 of the normalized flow distance, is much higher than for the other areas. This area corresponds to the mountainous region and the increased lateral discharge occurs due to snowmelt. The seasonal variation hillslope response of the Seki River is shown in Fig. 8(a,b,c,d). Fig. 8(a) shows that during the spring season, most of the river water comes from the area located at a normalized distance of 0.8–1.0 from the outlet due to snow melt, and Fig. 8(b) shows that during summer the response is directly proportional to the catchment area distribution. During autumn, most of the catchment response is due to the rainfall and is nearly proportional to the area function, but the downstream area has a slightly higher contribution than the rest of the catchment due to groundwater yield

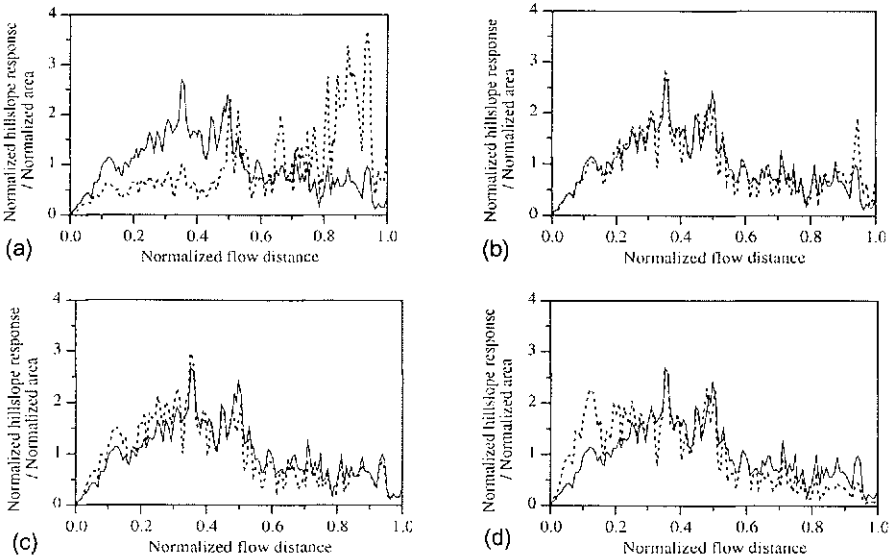


Fig. 8 Seasonal accumulative hillslope response distribution in the Seki River: (a) spring (March–May), (b) summer (June–August), (c) autumn (September–November) and (d) winter (December–February) (solid line: normalized accumulative area; dashed line: normalized accumulative hillslope response).

(Fig. 8(c)) and Fig. 8(d) shows that during winter the catchment area lying within a distance of 0–0.3 from the outlet has a very high contribution to the river flow. This shifting role of contribution from regions near to the outlet and further from the outlet can be explained by the alternating role of snow melt and groundwater discharge.

Instantaneous hillslope response distribution at the peak of the flood of 1993 in the Naka River is shown in Fig. 9(a). The flow contribution is mainly from the area at a normalized distance of 0.75–0.9 from the outlet. Nearly 50% of the runoff is generated from about 20% of the catchment area. This response is mainly due to the rainfall distribution in the catchment. The instantaneous hillslope response for the 1995 flood in the Seki River is shown in Fig. 9(b). The main contribution to the flow is from the area within a normalized distance of 0.5 from the catchment outlet, again as a result of the rainfall distribution.

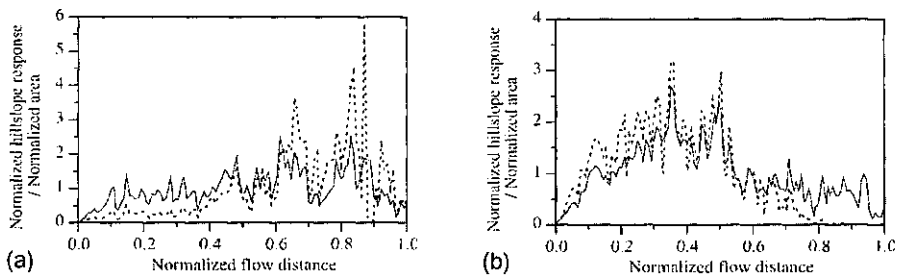


Fig. 9 Instantaneous hillslope response distribution: (a) Naka River, 1993 flood; (b) Seki river, 1995 flood. (solid line: normalized accumulative area; dashed line: normalized instantaneous hillslope response).

CONCLUSIONS

Model results are represented as normalized distributions with respect to flow distance, and, together with the area function, provide a means for interpreting spatial and seasonal hydrological response characteristics easily. Such information can be especially useful in implementing flood control measures such as surface retention within the catchment and water resources studies. The simplified modelling approach is efficient and requires only about 10 minutes for a one-year simulation with one-hour time steps on a UNIX workstation, facilitating repeated simulations for different land use and climatic condition scenarios.

REFERENCES

- Mesa, O. J. & Mifflin, E. R. (1986) On the relative role of hillslope and network geometry in hydrologic response. In: *Scale Problems in Hydrology* (ed. by V. K. Gupta, I. Rodriguez-Iturbe & E. Woods), 1–17. Reidel, Dordrecht, The Netherlands.
- Naden, P. S. (1992) Spatial variability in flood estimation for large catchments: the exploitation of channel network structure. *Hydrol. Sci. J.* 37(1) 53–71.
- Ni, G., Herath, S. & Musiak, K. (1994) Numerical simulation of hillslope infiltration and discharge into rivers. *Ann. J. Hydraul. Engng JSCE* 38, 191–196.
- Rinaldo, A., Rodriguez-Iturbe, I., Rigon, R., Ijjasz-Vasquez, E. & Bras, R. L. (1993) Self-organized fractal river networks. *Phys. Rev. Lett.* 70(6) 822–825.

- Robinson, J. S., Sivapalan, M. & Snell, J. D. (1995) On the relative roles of hillslope processes, channel routing, and network geomorphology in the hydrologic response of natural catchments. *Wat. Resour. Res.* 31(12) 3089–3101.
- Yang, D., Herath, S. & Musiak, K. (1997a) Analysis of geomorphologic properties extracted from DEMs for hydrologic modeling. *Ann. J. Hydraul. Engng JSCE* 41, 105–110.
- Yang, D., Herath, S. & Musiak, K. (1997b) Simulation of catchment rainfall-runoff using area function and tank model. *Proc. Ann. Conf. JSCE* 52(11), 324–325.